

PRELIMINARY COMMUNICATION

Three-dimensional reconstruction of port wine stain vascular anatomy from serial histological sections

Derek J Smithies^{†||}, Martin J C van Gemert^{†‡}, Marta K Hansen[§], Thomas E Milner[†] and J Stuart Nelson[†]

[†] Beckman Laser Institute and Medical Clinic, University of California, Irvine, USA

[‡] Laser Center, Academic Medical Center, Amsterdam, The Netherlands

[§] Department of Engineering, Harvey Mudd College, Claremont, California, USA

Received 8 May 1997

Abstract. Port wine stains (PWSs) treated with a flashlamp-pumped pulsed dye laser show a variability in clinical response that is incompletely understood. To identify any vascular structure that might adversely affect treatment response, we obtained a three-dimensional reconstruction of the vascular anatomy of a non-responsive, light-purple superficial PWS on the forearm. The reconstructed PWS consisted of multiple clusters of small diameter (10–50 μm) blood vessels. We propose that this and similar structures, which have not been identified in the literature, have limited the efficacy of laser therapy.

Further study is required to clarify the role of vessel clusters for laser treatment of PWSs, and the corresponding dosimetry necessary to clear non-responsive lesions. We expect that three-dimensional reconstruction of PWS vascular anatomy will provide the basis for (i) accurate PWS classification, (ii) guidance for selection of more effective laser dosimetry, and (iii) a standard against which to assess non-invasive diagnostic imaging techniques.

1. Introduction

Clinical response of port wine stains (PWSs) to laser therapy using currently accepted parameters (585 nm wavelength, 0.45 ms pulse duration, 5–10 mm spot diameter, single pulse) cannot be accurately predicted (Tan *et al* 1989, Alster and Wilson 1994, Morelli *et al* 1995). Extensive histological analysis (Barsky *et al* 1980), three-dimensional reconstruction of vascular anatomy (Braverman and Key-Yen 1983), classification (Ohmori and Huang 1981, Shakespeare and Carruth 1986), and analytical and computer simulations (Anderson and Parrish 1981, Smithies *et al* 1995, van Gemert *et al* 1997) have not provided a conclusive answer as to why some PWSs respond poorly to laser treatment.

The purpose of this paper is to present a method for obtaining a three-dimensional histological reconstruction of a PWS. We describe a novel anatomical vascular structure that might adversely affect treatment outcome when using currently accepted laser parameters.

2. Materials and methods

A three millimeter diameter punch biopsy was excised from an informed, consenting thirty-year-old Caucasian female with a non-responsive, light-purple superficial PWS on

|| Author to whom correspondence should be addressed. E-mail address: smithies@bli.uci.edu.

the forearm. The excised PWS tissue specimen was embedded in paraffin, cut in $6\ \mu\text{m}$ thick sections, and stained with hematoxylin and eosin. A colour video camera with a 640×480 element CCD array mounted on a microscope acquired images of seventy consecutive sections of the PWS tissue specimen. A $20\times$ magnification was selected to resolve individual blood vessels while requiring a minimum of three overlapping images to record an entire section in one composite image (figure 1). Provided operator error is eliminated, two images can be sufficient to generate a complete composite image. However, three images were always used to ensure that the entire histological section was recorded.

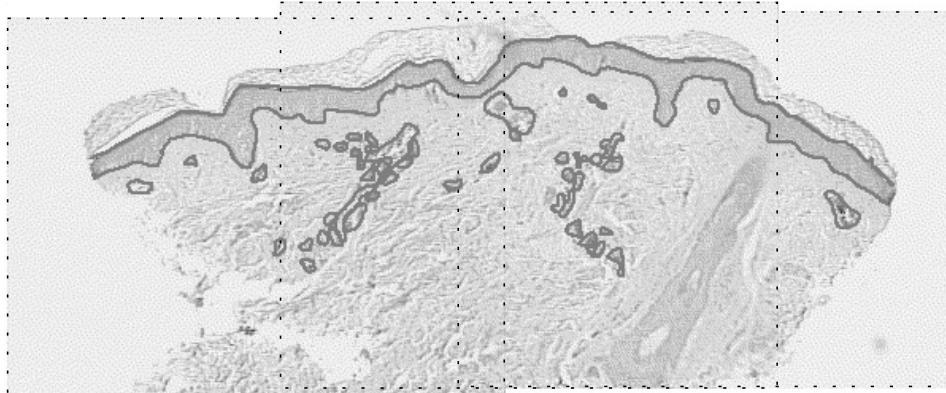


Figure 1. Composite image formed by combining three overlapping images of one histological section. The epidermis and vessels are outlined.

Interactive mouse-operated utilities were programmed for a commercial image-visualization package, AVS (Advanced Visual System, Waltham, MA), which has been described by Upson *et al* (1989). The programmed utilities (i) combined images, (ii) outlined and stored the position of the epidermal region and vessel circumference, and (iii) reconstructed the three-dimensional vasculature from the recorded position of the epidermis and vessels. The lines encompassing the epidermis and blood vessels for each composite image were rotated and translated so that the corresponding regions of consecutive sections coincided. From the entered lines, rotation and translation coordinates, the three-dimensional histological reconstruction was formed with standard linear algebra techniques. The reconstruction was rotated and dissected to view features of interest.

The average relative fractional blood volume was calculated from the entered lines, rotation and translation coordinates, and is the normalized plot of vessel area as a function of depth. The depth was taken as the minimum distance between the vessel centre and basal layer. The area of each vessel was calculated by counting the number of pixels required to fill the region delineated by the entered circumference.

3. Results

In figure 2, the image of a 2 mm (length) by 0.5 mm (width) by 1 mm (depth) region of the analysed PWS tissue specimen is shown from two points of view (figure 2(a) and (c)). In figure 2(b), a small region at the centre of the reconstructed three-dimensional vasculature was taken and shown at an enlarged scale. Large feeding vessels that connect the subcutaneous tissue to the superficial vascular plexus are indicated (FV in figure 2(c)). These vessels connect to many different points in the superficial vascular plexus and to

other feeder vessels. The spatial distribution of blood vessels is non-uniform and multiple connected clusters of small diameter ($10\text{--}50\ \mu\text{m}$) vessels may be distinguished (figure 2(b)). The ‘void’ on the right hand side of figure 2(a) and (c) is due to the presence of a hair follicle. Isolated features represent vessels that are located at the edge of the PWS tissue specimen and are present in only a few sections (figure 2(a) and (c)). The distinction between adjacent vessels is sometimes unclear when diameter and/or separation is less than $20\ \mu\text{m}$.

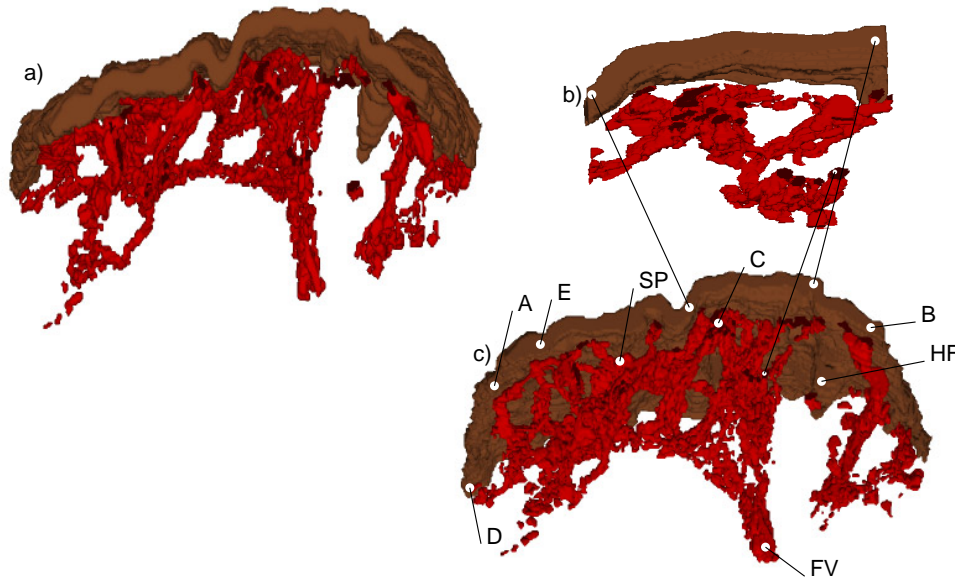


Figure 2. Three-dimensional histological reconstruction of epidermis and PWS vessels from 70 serial histological sections. Clusters (C) of small diameter vessels, epidermis (E), feeding vessels to deep plexus (FV), hair follicle (HF), and superficial plexus (SP) are observable. (a) Side view, which shows connections between three feeding vessels and superficial vascular plexus. (b) Perspective view of a small region at the centre of the reconstructed three-dimensional vasculature. (c) Perspective view of reconstructed three-dimensional vasculature. Distance AB = 1.9 mm, AD = 0.5 mm. Angle of view: 45° below (a).

The average relative fractional blood volume as a function of depth (figure 3) has a peak $200\ \mu\text{m}$ below the air–epidermis boundary. The three-dimensional histological reconstruction of the analysed PWS tissue specimen indicates a superficial lesion where virtually all of the dermal blood volume is within $500\ \mu\text{m}$ of the epidermal–dermal junction.

4. Discussion

The three-dimensional reconstruction technique presented here has provided a realistic representation of PWS vessel geometry, within the limitations of artefacts introduced by excision and processing of the tissue specimen. The reconstruction technique as implemented has minimal applicability as a routine diagnostic tool as approximately 50 h

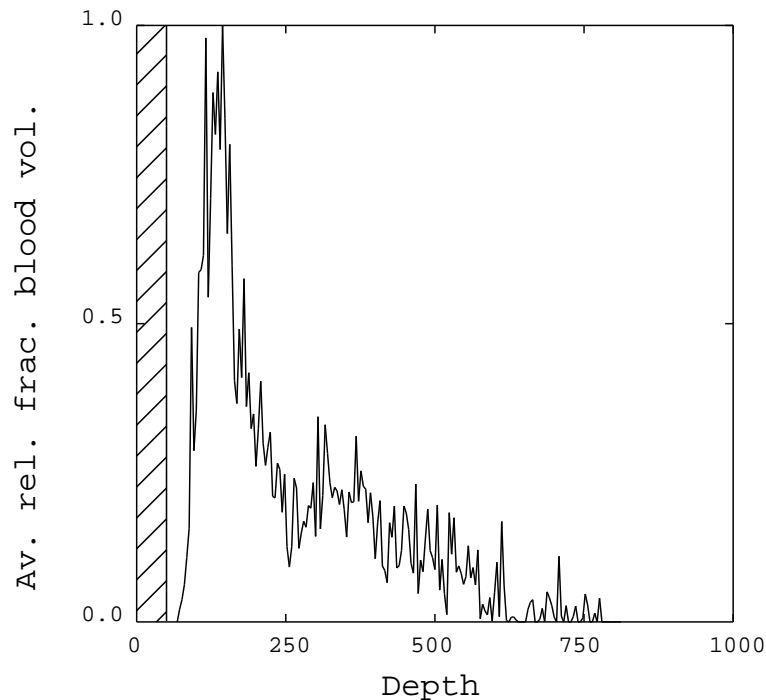


Figure 3. Average relative fractional blood volume as a function of depth within the analysed PWS tissue specimen. The epidermal region is indicated by the hatched rectangular area.

were required to enter the position and size of the vessels and epidermis for 70 consecutive histological sections. The technique is superior to standard histological analysis as the three-dimensional position of each vessel and epidermis is clear. Numerical analysis of the vessel size and position was carried out to give an accurate estimate of the average relative fractional blood volume as a function of depth. The PWS so analysed can then be classified, from which the appropriate laser dosimetry may be selected.

The three-dimensional histological reconstruction of PWS vascular anatomy revealed multiple clusters of small diameter (10–50 μm) blood vessels. We propose that this and similar structures, which have not been identified in the literature, may limit the efficacy of laser treatment of PWS. Analytical (Anderson and Parrish 1981), numerical (Pickering *et al* 1989) and Monte Carlo (Smithies and Butler 1995) modelling suggests that current laser treatment is adversely affected by small vessel conglomerates. First, heat deposition in individual vessels by light absorption in blood is significantly reduced by competition from the surrounding vasculature. Second, heat loss by thermal conduction, a significant effect for small diameter vessels, constrains the temperature increase as the heat generated is dissipated to surrounding dermal tissue. Consequently, few, if any, vessels within conglomerates will be photocoagulated, which may explain why this PWS was non-responsive to laser treatment.

Results from our three-dimensional reconstruction technique can provide a standard against which to assess non-invasive imaging techniques, such as transcutaneous microscopy (Shakespeare and Carruth 1986), infrared tomography (Milner *et al* 1995), and optical Doppler tomography (Chen *et al* 1997).

5. Conclusions

Further study is required to clarify the role of vessel clusters in laser treatment of PWSs, and corresponding dosimetry to clear non-responsive lesions. We expect three-dimensional reconstruction of PWS vessels will provide the basis for (i) accurate PWS classification, (ii) guidance for selection of more effective laser dosimetry, and (iii) a standard against which to assess non-invasive diagnostic imaging techniques.

Acknowledgments

Institutional support from the Department of Energy, the National Institutes of Health, and the Beckman Laser Institute and Medical Clinic Endowment is gratefully acknowledged (DJS, JSN). Support from research grants awarded by the Dutch Technology Foundation (STW grant AGN 55-3906), the Academic Medical Center (MJCvG), the Whitaker Foundation (WF-21025)(TEM, MKH), and the Institute of Arthritis and Musculoskeletal and Skin Diseases (1R29-AR41638-01A1 and 1R01-AR42437-01A1) at the National Institutes of Health (JSN,TEM) is also gratefully acknowledged.

References

- Alster T S and Wilson F 1994 Treatment of port-wine stains with the flashlamp-pumped pulsed dye laser: extended clinical experience in children and adults *Ann. Plastic Surg.* **32** 478–84
- Anderson R R and Parrish J A 1981 Microvasculature can be selectively damaged using dye lasers: A basic theory and experimental evidence in human skin *Lasers Surg. Med.* **1** 293–76
- Barsky S H, Rosen S, Geer D E and Noe J M 1980 The nature and evolution of port wine stains: A computer-assisted study *J. Investig. Dermatol.* **74** 154–7
- Braverman I M and Key-Yen A 1983 Ultrastructural and three-dimensional reconstruction of several macular and papular telangiectases *J. Investig. Dermatol.* **81** 489–97
- Chen Z, Milner T E, Dave D and Nelson J S 1997 Optical doppler tomographic imaging of fluid flow velocity in highly scattering media *Optics Lett.* **22** 64–6
- Milner T E, Goodman D M, Tanenbaum B S and Nelson J S 1995 Depth profiling of laser-heated chromophores in biological tissues by pulsed photothermal radiometry *J. Opt. Soc. Am. A* **12** 1479–88
- Morelli J G, Weston W L, Huff J C and Yohn J J 1995 Initial lesion size as a predictive factor in determining the response of port-wine stains in children treated with the pulsed dye laser *Arch. Pediatr. Adolesc. Med.* **149** 1142–44
- Ohmori S and Huang C K 1981 Recent progress in the treatment of port-wine staining by the argon laser: some observations on the prognostic value of relative spectro-reflectance (RSR) and the histological classification of the lesions *Br. J. Plastic Surg.* **34** 249–57
- Pickering J W, Butler P H, Ring B J and Walker E P 1989 Computed temperature distributions around ectatic capillaries exposed to yellow (578 nm) laser light *Phys. Med. Biol.* **34** 1247–58
- Shakespeare P G and Carruth J A S 1986 Investigating the structure of the port-wine stain by transcutaneous microscopy *Lasers Med. Sci.* **1** 107–9
- Smithies D J and Butler P H 1995 Modelling the distribution of laser light in port-wine stains with the Monte Carlo method *Phys. Med. Biol.* **40** 701–33
- Smithies D J, Butler P H, Day W T and Walker E P 1995 The effect of the illumination time when treating port-wine stains *Lasers Med. Sci.* **10** 93–104
- Tan O T, Sherwood K and Gilchrist B A 1989 Treatment of children with port-wine stains using the flashlamp-pulsed tuneable dye laser *New England J. Med.* **320** 416–21
- Upson C, Faulhaber T, Kamins D, Schlegel D, Vroom J, Gurwitz R and van Dam A 1989 The Application Visualization System: A computational environment for scientific visualization *IEEE Comput. Graph. Applic.* **9** 30–42
- van Gemert M J C, Smithies D J, Verkruysse W, Milner T E and Nelson J S 1997 Wavelengths for port wine stain laser treatment: influence of vessel radius and skin anatomy *Phys. Med. Biol.* **42** 41–50